JOURNAL OF VIROLOGY, June 1995, p. 3838–3847 Vol. 69, No. 6
0022-538X/95/$04.00+0
Copyright © 1995, American Society for Microbiology

Selective Depletion of Stored Calcium by Thapsigargin Blocks Rotavirus Maturation but Not the Cytopathic Effect

FABIAN MICHELANGELI,[1]* FERDINANDO LIPRANDI,[2] MARIA ELENA CHEMELLO,[1] MAX CIARLET,[2] AND MARIE-CHRISTINE RUIZ[1]

Laboratorio de Fisiología Gastrointestinal[1] and Laboratorio de Biología de Virus,[2] Instituto Venezolano de Investigaciones Científicas, Caracas 1020A, Venezuela

Received 27 July 1994/Accepted 16 February 1995

Rotavirus matures inside the endoplasmic reticulum (ER), a site of intracellular calcium storage. Total cell Ca^{2+} depletion has been shown to impair virus maturation, arresting this process at the membrane-enveloped intermediate form following its budding into the ER. On the other hand, rotavirus infection leads to an increase in the internal Ca^{2+} concentration ($[Ca^{2+}]_i$) and sequestered Ca^{2+} pools. We have used thapsigargin, an inhibitor of the Ca^{2+}-ATPase of the ER, to release stored Ca^{2+} and to study its role in rotavirus morphogenesis and cytopathic effect. Thapsigargin (0.1 to 1 μM) released stored Ca^{2+} from MA-104 cells, as measured by chlorotetracycline fluorescence. The concentration of cytoplasmic Ca^{2+}, measured with fura2, increased in infected cells whether treated or not with thapsigargin. Infectivity was decreased dose dependently by thapsigargin (3 log units at 0.25 to 1 μM). In infected cells treated with thapsigargin, glycosylation of VP7 and NS28 was inhibited. Electron microscopy of infected cells treated with thapsigargin showed normal synthesis of viroplasm. However, only membrane-enveloped, not double-shelled, particles could be observed within the ER. The conformation of VP7 in infected cells treated with thapsigargin appeared to be altered, as suggested by decreased immunofluorescence reactivity with monoclonal antibodies to highly conformation-dependent VP7 epitopes. The progression of cell death in infected cells, as measured by penetration of ethidium bromide, was not affected by thapsigargin. These results indicate that rotavirus maturation depends on a high sequestered $[Ca^{2+}]$, specifically in the ER. Cell death is the result of the accumulation of a viral product and is not related to the production of infective particles. This viral product(s) may be responsible for the increase in $[Ca^{2+}]_i$, which in turn leads to cell death.

Rotaviruses are nonenveloped, double protein capsid viruses belonging to the *Reoviridae* family. They contain an 11-segment, double-stranded RNA genome that codes for six structural and five nonstructural proteins. The single capsid structure is formed in the cytoplasm, a medium characterized by a low Ca^{2+} concentration ($[Ca^{2+}]$), at special areas termed the viroplasm. Then, the single capsid structure buds into the endoplasmic reticulum (ER), forming a transiently enveloped viral particle. This includes the outer capsid proteins VP7 and VP4, forming a hetero-oligomeric complex with NS28 (NSP4), a nonstructural, ER-resident transmembrane protein (23, 29). The maturation of the particles to produce infectious viruses is thought to involve the loss of lipid and protein components of the acquired ER membrane and the nonstructural protein NS28 and the rearrangement of the outer capsid proteins VP4 and VP7 by an as yet undefined mechanism. In fact, an alternative assembly pathway by which subviral particles acquire the outer capsid proteins, involving transmembrane transport without the enveloped stage, has been proposed (36).

Calcium plays an important role all during the rotavirus cycle in the host cell. The stability of the double-shelled particle depends on the presence of Ca^{2+} (8), which appears to be an integral part of the rotavirus virion (33). A conformational change in VP7 induced by Ca^{2+} chelation has been invoked as being responsible for decapsidation (11). The maturation process has also been shown to be Ca^{2+} dependent; omission of Ca^{2+} from the culture medium stopped virus synthesis at the single-shell step (33, 34), whereas total cell Ca^{2+} depletion, achieved by using the Ca^{2+} ionophore A23187 and EGTA (ethylene glycol tetraacetic acid), arrested maturation, leading to an accumulation of membrane-enveloped viral particles within the cisternae of the ER (30).

These changes were concomitant with, and perhaps due to, a blockade of glycosylation processing of VP7 and NS28 and the formation of anomalous hetero-oligomeric protein complexes during the maturation process. These observations have been interpreted as being the result of Ca^{2+} depletion from the ER (29, 30). However, both cytoplasmic and stored Ca^{2+} concentrations increase in the course of viral infection (26). We have proposed that the sustained elevation of the cytoplasmic Ca^{2+} concentration is responsible for the cytopathic effect of the virus. Treatment with ionophore- and Ca^{2+}-free medium containing EGTA (30) should affect every Ca^{2+} compartment in the cell, making the interpretation uncertain. In this study, we have used thapsigargin, a sesquiterpene lactone derived from *Thapsia garganica*, an inhibitor of the ER Ca^{2+}-ATPase (37, 38), to selectively deplete the ER Ca^{2+} stores. With the aid of this agent, we have studied the role of Ca^{2+} concentration in different subcellular compartments in virus maturation and cell death. We have found that thapsigargin arrests rotavirus maturation at the membrane-enveloped stage without impairing cell death. We believe that the first process depends on a high Ca^{2+} concentration in the cisternae of the ER and that the cytopathic effect depends on an elevated Ca^{2+} concentration in the cytosol.

* Corresponding author. Mailing address: IVIC, Apartado 21827, Caracas 1020A, Venezuela. Phone: (582) 5011396. Fax: (582) 5727446 or (582) 5011093. Electronic mail address: fabian@cbb.ivic.ve.

MATERIALS AND METHODS

Cell cultures and virus infection. Fetal rhesus monkey kidney cells (MA-104) were used throughout. Cells were grown and maintained as previously described

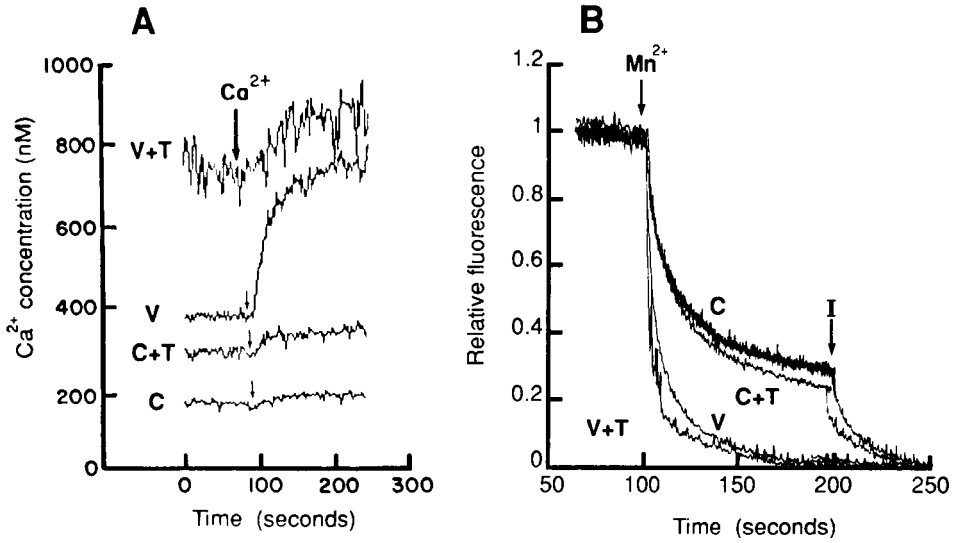

FIG. 1. Effect of thapsigargin (1 μM) on virus-induced changes in intracellular Ca^{2+} concentration and membrane permeability in MA-104 cells. Cells were exposed to thapsigargin (T) at 1 h postinfection. Mock- (C) or virus-infected (V) cells not treated with thapsigargin remained as controls. Measurements were performed at 10 h postinfection. (A) Ca^{2+} concentration was determined by fura2 fluorescence at 340 and 380 nm (excitation wavelengths), and Ca^{2+} permeability was evaluated by the initial change in Ca^{2+} concentration after the addition of a 5 mM Ca^{2+} pulse (arrows) to the incubation medium, which initially contained 1 mM Ca^{2+} (see text). A representative experiment of a series of five is shown. (B) Plasma membrane permeability to Ca^{2+} was determined by using Mn^{2+} as a surrogate for Ca^{2+}. The quenching of fura2 fluorescence induced by addition of 0.5 mM Mn^{2+} (arrow) was measured at an excitation wavelength of 360 nm. Relative fluorescence corresponds to the normalized fluorescence, taking initial values as maximal and ionomycin (I; 10 μM) values as minimal (see text). A representative experiment of a series of three is shown.

(26). In some experiments, confluent monolayers of the colonic cancer cell lines HT29 and Caco2 were used and cultured as for MA-104 cells. The OSU strain of porcine rotavirus was used in all experiments. Quantification of the infectivity of virus preparations was done by an immunofluorescence staining technique in microplates or a plaque assay (21). The conditions of infection were as follows. Virus preparations treated with trypsin (10 μg/ml, 1 h, 37°C) were added to confluent monolayers of cells which had been washed three times with phosphate-buffered saline (PBS). The time of virus addition was taken as time zero for all experiments. After 1 h of adsorption at 37°C, the cells were washed twice with PBS and replenished with maintenance medium (minimal essential medium [MEM]). Fetal calf serum (1%) was added to the maintenance medium except when infectivity was to be measured. A multiplicity of infection of 10 immunochemical fluorescence units per cell was used in all experiments. Thapsigargin was added at 1 to 4 h postinfection.

Determination of intracellular Ca^{2+} concentration. The intracellular calcium concentration ($[Ca^{2+}]_i$) was measured by using the fluorescent indicator fura2, which was incorporated intracellularly as its acetoxy-methyl ester (fura2-AM). Cell monolayers were trypsinized, washed by centrifugation, and resuspended in MEM at an approximate concentration of 2×10^6 cells per ml. For each measurement, aliquots of cell suspensions were individually incubated with 10 μM fura2-AM for 30 min at 37°C in a medium containing (in millimolar): NaCl, 132.4; KCl, 5; Na_2HPO_4, 5; NaH_2PO_4, 1.2; $CaCl_2$, 1; $MgCl_2$, 0.8; pyruvate, 1.0, and 1% (wt/vol) albumin. After loading, cells were washed twice by centrifugation to remove extracellular fura2-AM and resuspended in 1.2 ml of the same medium without albumin. Fluorescence was measured at 37°C in a spectrofluorometer (Photon Technology International) equipped with a stirrer and temperature control. The excitation wavelengths were 340 and 380 nm and were alternated by computer control, allowing acquisition of one pair of data per second. The emission was fixed at 510 nm. The ratio of the fluorescent signals measured at 340 and 380 nm was computer determined. The intracellular free Ca^{2+} concentration was evaluated by the method of Grynkiewiecz et al. (16), with an apparent K_d for fura2-Ca of 224 nM. The maximal fluorescence ratio (R_{max}) was determined by addition of digitonin (50 μg/ml) to permeabilize the cells, and the minimal fluorescence ratio (R_{min}) was determined by the subsequent addition of 20 mM EGTA (16). $[Ca^{2+}]_i$ was calculated by the equation $[Ca^{2+}]_i = K_d\,[(R - R_{min})/(R_{max} - R)] \times (Sf2/Sb2)$, where R is the fluorescence ratio at any given time and Sf2 and Sb2 are the fluorescence intensities of the free and bound forms of fura2 at the 380-nm excitation wavelength, respectively.

Assessment of membrane Ca^{2+} permeability. (i) Step change in extracellular Ca^{2+} concentration. The relative Ca^{2+} permeability of control and virus-infected cells was evaluated by imposing a step increase in the extracellular Ca^{2+} concentration and measuring the rate of change in $[Ca^{2+}]_i$ during the first few seconds (26). This change is the result of net Ca^{2+} flux between the cytoplasm and outside and between the cytoplasm and Ca^{2+}-sequestering organelles. However, the elevation in $[Ca^{2+}]_i$ during the first few seconds (with a linear slope) should be a measurement of unidirectional Ca^{2+} flux and therefore of calcium permeability.

(ii) Mn^{2+} influx. The rate of quenching of fura2 fluorescence by Mn^{2+} was also used to estimate plasma membrane permeability to Ca^{2+} (24) and the effect of rotavirus infection on this parameter (26). The measurements were made at excitation and emission wavelengths of 360 and 510 nm, respectively, wave-

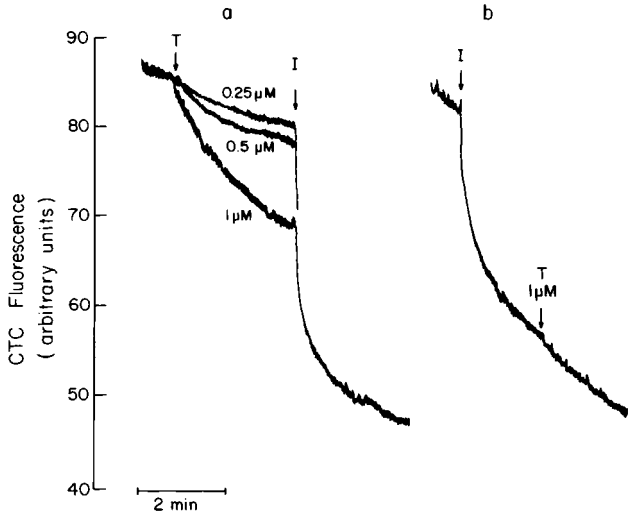

FIG. 2. Effect of the addition of thapsigargin on CTC efflux of preloaded, noninfected MA-104 cells, as a measurement of intracellular Ca^{2+} pools. Trypsinized cells were incubated with CTC (100 μM) for 1 h at 37°C. Fluorescence was measured in CTC-free medium (see text). (a) Addition of different concentrations of thapsigargin (T), 0.25, 0.5, and 1 μM, induced a dose-dependent decrease in fluorescence, which was taken to a minimal level by ionomycin (I, 10 μM). Traces corresponding to the different concentrations are superimposed on the graph. (b) Previous addition of ionomycin precluded the effect of further addition of thapsigargin. A representative experiment of a series of three is shown.

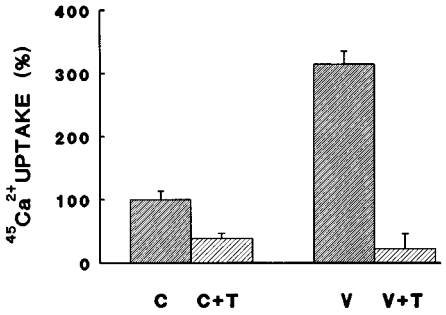

FIG. 3. Intracellular Ca^{2+} pools evaluated by $^{45}Ca^{2+}$ uptake in control (C) and rotavirus-infected (V) cells in the presence (T) or absence of thapsigargin. Thapsigargin (1 μM) was added at 1 h postinfection, and measurements were performed at 8 h postinfection. The time of uptake was 20 min. Values are from one experiment representative of three and correspond to the mean ± standard error of the mean (SEM) of measurements in four different wells in each condition, normalized to controls. The effect of thapsigargin was statistically significant for comparisons between thapsigargin-treated and untreated mock- and virus-infected cells ($n = 3$ in three experiments with four replicates each; $P < 0.001$ for all cases, unpaired t test).

lengths at which fura2 fluorescence is independent of Ca^{2+} concentration (16). We normalized the fluorescence to the initial intensity just before the addition of Mn^{2+} (100%). Ionomycin was added to obtain the fully quenched value that was taken as basal (0%). The slope was related to the membrane permeability to Mn^{2+} and, hence, Ca^{2+}.

Estimation of stored Ca^{2+} pools. (i) CTC efflux. To evaluate the mobilization of stored Ca^{2+} by thapsigargin, chlorotetracycline (CTC) efflux was measured. This indicator forms an amphipatic complex with Ca^{2+} that is in equilibrium across the different compartments of the cell. The complex partitions into both the nonpolar phase of cell membranes and aqueous compartments. The Ca-CTC complex fluoresces only in nonpolar media such as membranes. As the K_d for this complex is in the millimolar order (5), CTC senses only compartments of high Ca^{2+} accumulation (6, 10). A release of Ca^{2+} from these compartments by agonists or thapsigargin induces a shift in the equilibrium, resulting in the efflux of the Ca-CTC complex from the membrane and therefore a decrease in fluorescence (6, 25, 37). Trypsinized cell monolayers were washed by centrifugation, resuspended in MEM (2×10^6 cells per ml), and incubated in the presence of 100 μM CTC for 30 min at 37°C. The cells were washed by centrifugation to remove extracellular fluorophore and resuspended in 1.2 ml of a medium containing (in millimolar): NaCl, 132.4; KCl, 5; Na_2HPO_4, 5; NaH_2PO_4, 1.2; $CaCl_2$, 1; $MgCl_2$, 0.8; and pyruvate, 1.0. The efflux of CTC was measured in the fluorometer at 398 and 510 nm for excitation and emission wavelengths, respectively.

(ii) $^{45}Ca^{2+}$ uptake. Cell monolayers were grown to confluence in 24-well Linbro plates and infected as described above. At 8 to 10 h postinfection, maintenance medium was removed and replaced by 200 μl of MEM containing $^{45}Ca^{2+}$ (1 μCi per well). In preliminary experiments, we measured uptake from 0 to 30 min and found out that at 10 min it had already reached a plateau. Therefore, uptake was stopped after 20 min by washing the cells four times by immersion in ice-cold PBS. After drying, cells were dissolved with 0.25 ml of NaOH (0.1 N). After neutralization with HCl, radioactivity was determined by liquid scintillation counting. As the number of cells per well was found to be constant, uptake values for single experiments are expressed as a percentage of the total counts per minute per well of mock-infected cells.

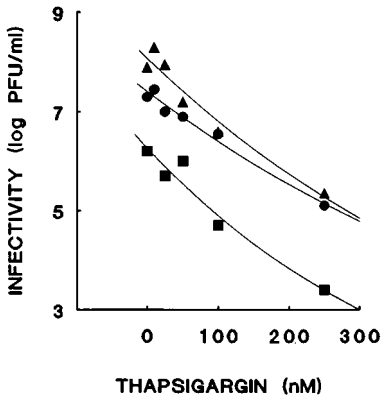

FIG. 4. Dose-dependent inhibition of rotavirus infectivity by thapsigargin (0 to 250 nM) in different cell lines. Thapsigargin was added at 4 h postinfection. Infectivity was measured at 8 h postinfection in MA104 (triangles), HT29 (circles), and Caco2 (squares) cells. A representative experiment of a series of four for MA-104 and two each for HT29 and Caco2 cells is shown.

Labeling and analysis of proteins by PAGE and Endo-H treatment. Confluent monolayers of MA-104 cells were infected and overlaid with methionine-free MEM. At 4 h postinfection, the cell cultures were pulsed for 2 h with 50 μCi of [^{35}S]methionine per ml. Cells were collected from the flask with a rubber policeman, washed in PBS, and lysed for 10 min on ice with lysis buffer (0.01 M Tris-HCl, 0.1 M NaCl, 2 mM phenylmethylsulfonyl fluoride, and 1% Nonidet P-40). After pelleting the nuclei at 2,000 × g for 3 min, supernatants were collected and stored frozen for electrophoretic analysis. Sodium dodecyl sulfate-polyacrylamide gel electrophoresis (SDS-PAGE) on 10% polyacrylamide gels and autoradiography were performed as described by Gorziglia et al. (15). In some experiments, methionine-labeled cell lysates were digested with endo-β-*N*-acetylglucosaminidase (Endo-H; H Bio Labs) before PAGE. Denatured samples (10 min at 100°C in 0.5% SDS–1% β-mercaptoethanol) were digested with 1 μl of Endo-H (1 h at 37°C) in 0.05 M sodium citrate (pH 5.5).

Electron microscopy of infected cells. MA-104 cells were infected as above, treated or not with thapsigargin, fixed at 8 h postinfection in 2.5% glutaraldehyde in 0.1 M cacodylate buffer, and postfixed with osmium tetroxide (1%). Fixed cells were embedded in Epon, sectioned with diamond knives (Instituto Venezolano de Investigaciones Científicas), and viewed under the electron microscope after staining with uranyl acetate and lead citrate.

Immunofluorescence assay on infected cells with MAbs against VP4, VP6, and VP7. Confluent monolayers of MA-104 cells grown in microtiter plates and infected as described above were maintained at 37°C in MEM with or without thapsigargin (1 μM) or tunicamycin (5 μg/ml). Cells were washed in PBS and fixed at 18 h postinfection, either with methanol (20 min at 4°C) or with paraformaldehyde with subsequent treatment with Triton X-100, as described by Dormitzer et al. (12). The following monoclonal antibodies (MAbs) were used for immunofluorescence staining: MAb 4B2D2, directed against a common group A antigen of VP6 (20); MAb 5G7, directed against VP4 (VP8 subunit) of the OSU strain (21); and MAbs 1C3 and 1C10, directed against VP7. These two antibodies exhibit a G5 serotype-specific pattern of reactivity by neutralization and enzyme-linked immunosorbent assay (ELISA) and select neutralization escape mutants of the OSU strain with amino acid substitutions at positions 94 and 96, respectively (7). After incubation with the antibodies (1 h at 37°C), the cells were washed, and the antibodies were developed with an anti-mouse immunoglobulin G-fluorescein isothiocyanate-conjugated antiserum (Sigma) for 2 h at 37°C. Fluorescence was observed and photographed with an inverted fluorescence microscope (Nikon Diaphot TMD; Kodak film TMax 3200).

Quantification of cell death by permeabilization to ethidium bromide. Cell death after rotavirus infection was determined in confluent cell monolayers grown in 24-well Linbro plates by using the nucleic acid-binding compound ethidium bromide (32). At different times postinfection, control and infected monolayers were incubated with 50 μM ethidium bromide in PBS for 5 min. The medium was then removed, and the fluorescence of the monolayer was measured with an inverted microscope (Nikon Diaphot TMD) equipped with a P1 microphotometry system. The epifluorescence system had an excitation filter (510 to 560 nm), a barrier filter (590 nm), and a dichroic mirror (580 nm). The fluorescence of the central area of the well (2.5 mm in diameter) was measured with a 4× objective. The total red emitted fluorescence was a function of the number of cells permeable to ethidium bromide in the monolayer. This number was used as an index of cell death and normalized after total permeabilization with digitonin (40 μg/ml).

RESULTS

Effect of thapsigargin on Ca^{2+} homeostasis of control and virus-infected MA-104 cells. (i) Ca^{2+} concentration and membrane permeability. In preliminary control experiments, thapsigargin induced a transient increase in the cytoplasmic free Ca^{2+} concentration in noninfected MA-104 cells. The response was characterized first by a rapid elevation in Ca^{2+} concentration, decaying to a sustained level above the basal concentration (results not shown). This effect has been observed in many cell types and has been associated with the inhibition of the ER Ca^{2+}-ATPase, the passive release of stored Ca^{2+}, and a subsequent entry of Ca^{2+} (37).

We then studied the effect of thapsigargin on the Ca^{2+} concentration and on membrane permeability of infected cells that had been exposed to this agent from 1 h postinfection. At 10 h postinfection, an increase in the basal Ca^{2+} concentration was observed in virus-infected cells (Fig. 1A), confirming our

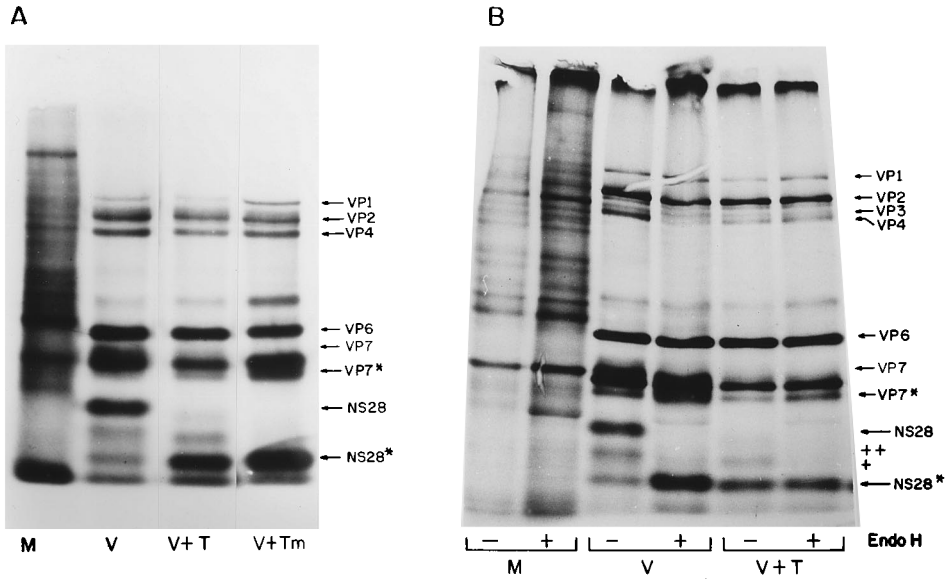

FIG. 5. (A) Effect of thapsigargin (1 μM) and tunicamycin (5 μg/ml) on rotavirus protein synthesis in infected MA-104 cells (V) analyzed by SDS-PAGE. Thapsigargin (V+T) or tunicamycin (V+Tm) was added at 1 h postinfection, and the cells were labeled with [^{35}S]methionine for 2 h before harvesting at 6 h postinfection. (B) SDS-PAGE analysis of labeled cell lysates of mock-infected cells (M) or rotavirus-infected cells (V) previously treated (V+T) or not (V) with 1 μM thapsigargin (added at 1 h postinfection) and digested (+) or not (−) with Endo-H. The + and ++ in the right margin mark NS28 glycosylated at one or two sites, respectively, which disappear after Endo-H treatment. Unglycosylated forms of viral proteins are marked by *.

earlier findings (26). The increase in Ca^{2+} concentration induced by virus infection was higher in the presence of thapsigargin. This agent alone also induced a moderate increase in Ca^{2+} concentration in mock-infected cells.

Rotavirus infection induced an increase in membrane Ca^{2+} permeability. This was observed with the Ca^{2+} pulse method as well as with Mn^{2+} influx (Fig. 1A and B). A change in the extracellular Ca^{2+} concentration induced an augmentation in fura2 fluorescence, the slope of which was higher in infected cells (Fig. 1A). Similarly, the rate of Mn^{2+} quenching of intracellular fura2 fluorescence was increased in rotavirus-infected cells and even further increased in those that had been exposed to thapsigargin (Fig. 1B). Addition of ionomycin to increase Ca^{2+} permeability induced a further decrease in fluorescence in control cells but not in virus-infected cells. These results confirm the effect on calcium permeability caused by viral infection shown earlier (26). Furthermore, the effects on permeability induced by rotavirus infection persist in the presence of thapsigargin. Thapsigargin by itself (in mock-infected cells) induced an increase in Ca^{2+} permeability and concentration. This may be the cause of the higher Ca^{2+} concentrations observed in virus-infected cells treated with thapsigargin.

(ii) Ca^{2+} mobilization from stores. The mobilization of Ca^{2+} from stores by thapsigargin was dose dependent, as seen from a decrease in CTC fluorescence of preloaded cells (Fig. 2a). Only a fraction of sequestered Ca^{2+} was released by the maximal concentration of thapsigargin used (1 μM), since ionomycin, a Ca^{2+} ionophore, was able to cause a further decrease. Thapsigargin depleted stores which were also sensitive to ionomycin, since the addition of thapsigargin after the ionophore did not induce further CTC efflux (Fig. 2b).

Estimation of Ca^{2+} pools in mock- and virus-infected cells was performed by measuring $^{45}Ca^{2+}$ uptake over 20 min. At 20 min, uptake reaches a plateau and is in equilibrium with the different calcium pools of the cell (26). The larger part of $^{45}Ca^{2+}$ uptake must be considered to be due to Ca^{2+} sequestered in organelles, since the contribution of cytoplasmic Ca^{2+} is rather small. As the results were similar at 6, 8, and 10 h postinfection, we only present those obtained at 8 h postinfection (Fig. 3). $^{45}Ca^{2+}$ uptake at this time was on average threefold higher in virus-infected cells. Thapsigargin (1 μM) decreased $^{45}Ca^{2+}$ uptake in both mock- and virus-infected cells ($P < 0.001$, unpaired t test; $n = 3$ in three experiments with four replicates each). Therefore, this agent inhibits the increase in sequestered Ca^{2+} pools induced by infection. The thapsigargin-sensitive compartment, probably the ER, is the one increased during rotavirus infection.

Viral maturation in the presence of thapsigargin. (i) Infectivity of rotavirus particles produced in the presence of thapsigargin. Thapsigargin induced a dose-dependent inhibition of the production of infectious virus in MA-104, HT29, and Caco2 cells. At a concentration of 250 nM to 1 μM, this was on the order of 3 log units for all cell lines (Fig. 4). Similar results were obtained when the drug was added up to 4 h postinfection. Thapsigargin by itself did not modify the determination of infectivity; incubation of infected cell lysates with the agent for 1 h at 37°C before titration did not affect the results.

Therefore, the modification of Ca^{2+} compartments inside the cell induced by thapsigargin inhibited infectious rotavirus particle production at some point in the viral replication cycle.

(ii) Analysis of protein synthesis by SDS-PAGE. Cellular protein synthesis in mock-infected MA-104 cells was not apparently affected by thapsigargin during the labeling period studied (from 6 to 8 h postinfection; results not shown). In infected cells, the only viral proteins whose pattern of electrophoretic migration was modified were NS28 and VP7. Treatment with thapsigargin blocked the synthesis of the mature form of NS28, with the concomitant accumulation of a protein product of about 20 kDa. Treatment with tunicamycin, a known glycosylation inhibitor, during infection completely inhibited the synthesis of the mature form of NS28, which was present only as the unglycosylated 20-kDa protein. Digestion of the labeled cell lysates with Endo-H induced the complete elimination of the 28-kDa band of NS28 and an increase in the

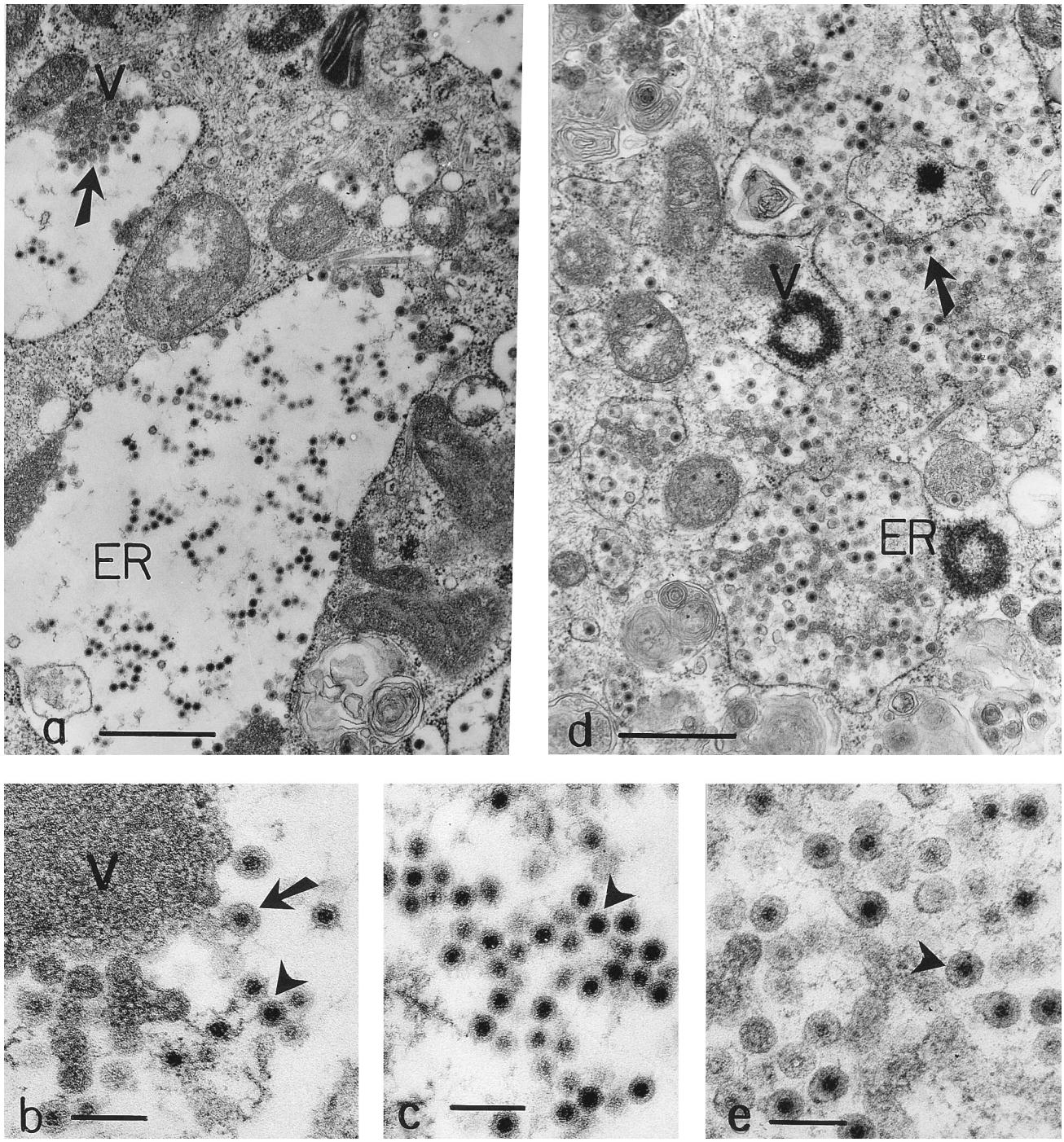

FIG. 6. Effect of thapsigargin (1 μM) on the ultrastructure of rotavirus-infected MA-104 cells. Cells were fixed at 8 h postinfection in 2.5% glutaraldehyde in 0.1 M cacodylate buffer and postfixed with osmium tetroxide (1%). Single-shelled particles can be observed emerging from the viroplasm, budding into the ER, and covering themselves with the ER membrane (a and b, arrows). These membrane-enveloped particles can be seen near the viroplasmic structure or in proximity to the ER membrane. Towards the center of dilated cisternae, double-shelled particles devoid of enveloping membrane can be observed (c, arrowheads). In infected cells treated with thapsigargin from 1 h postinfection, viroplasmic inclusions and images of particle budding into ER are also observed (d, arrows), but there is an abnormal accumulation of membrane-enveloped particles within the cisternae of the ER (e, arrowheads). V, viroplasmic inclusions. Bars: (a and d) 100 nm; (b, c, and e) 200 nm.

20-kDa band (Fig. 5B). Comparison of the different electrophoretic patterns with thapsigargin, Endo-H, and tunicamycin treatments leads to the conclusion that thapsigargin impairs the glycosylation of NS28 (Fig. 5A and B). Intermediate products of lower molecular weight that may correspond to NS28 glycosylated at one or two positions disappeared after digestion of the labeled cell lysate with Endo-H. This effect was observed in infected cells whether treated or not with thapsigargin (Fig. 5B).

The analysis of changes in the electrophoretic mobility of

TABLE 1. Recognition of viral protein by MAbs as evidenced by immunofluorescence[a]

MAb (specificity)	Fluorescence intensity						
	Methanol-fixed cells			Paraformaldehyde-fixed cells			
	Uninfected	Infected	Infected and thapsigargin treated	Uninfected	Infected	Infected and thapsigargin treated	Infected and tunicamycin treated
4B2D2 (VP6)	−	+++	+++	−	++++	++++	+++
5G7 (VP4)	−	+++	+++	−	++++	++++	+++
1C3 (VP7)	−	−	−	−	+++	+	+
IC10 (VP7)	−	−	−	−	+++	+	+

[a] MA-104 cell monolayers grown in 96-well plates were infected with trypsin-activated strain OSU and maintained at 37°C. At 1 h postinfection, thapsigargin (1 μM) or tunicamycin (5 μg/ml) was added. At 18 h postinfection, the cells were washed in PBS and fixed either with methanol or paraformaldehyde, and fluorescence was developed as described in Materials and Methods. Intensity of fluorescence is expressed semiquantitatively, from ++++ (maximal) to − (no specific signal).

VP7 was made difficult by the migration of several viral proteins very close to each other, VP7, NS35, NS34, and the nonglycosylated form of VP7. However, we can observe a band that disappears after treatment with tunicamycin (Fig. 5A, lane V+Tm) and with Endo-H (Fig. 5B, lane V+) that should correspond to VP7. Concomitantly, an increase in the thickness of a lower-molecular-weight band could be observed after treatment with tunicamycin or digestion with Endo-H. This suggests that this band corresponds to the unglycosylated form of VP7 (Fig. 5A and B, VP7*). The disappearance of the putative glycosylated VP7 band was evident after treatment with thapsigargin (Fig. 5A, lane V+T, and 5B, lane V+T−), suggesting that this agent affects the glycosylation of VP7. However, accumulation of VP7* did not occur under these conditions. It is possible that unglycosylated VP7 undergoes fast degradation (33). Together, these results indicate that thapsigargin, like tunicamycin, inhibits the glycosylation process of both NS28 and VP7.

(iii) Ultrastructure of the particles in the infected cell. The effect of thapsigargin on the viral assembly process was studied in MA-104 cells fixed at 6 h postinfection (Fig. 6). At this point, cells not treated with thapsigargin present electron-dense structures in the cytoplasm, corresponding to viroplasm, in close apposition to a dilated rough ER (Fig. 6a). Single-shelled particles were observed emerging from the viroplasm, budding into the ER, and acquiring the ER membrane during this process. These membrane-enveloped particles were seen near the viroplasmic structure or in proximity to the ER membrane. Towards the center of dilated cisternae, double-shelled particles devoid of enveloping membrane were present (Fig. 6b and c). In infected cells treated with thapsigargin from 1 to 6 h postinfection, viroplasmic inclusions and images of particle budding into the ER were also observed (Fig. 6d). In addition, there was an abnormal accumulation of membrane-enveloped particles within the cisternae of the ER (Fig. 6d). In this case, a small number of nonenveloped particles were found. It has been proposed that the membrane-enveloped stage is a transitory one and that loss of this membrane results in the assembly of the mature particle (13). Thapsigargin therefore seems to arrest the morphogenesis of rotavirus at the membrane-enveloped stage.

(iv) Recognition of viral proteins by MAbs. To evaluate the possible alteration in the conformation of VP7 in infected cells treated with thapsigargin, we tested whether epitopes on this protein, which are known to be part of a highly conformation-dependent antigenic domain, would be preserved in thapsigargin-treated cells. The reactivity of two neutralizing MAbs specific for VP7 of the OSU strain was tested by immunofluorescence. We also used an anti-VP6 and an anti-VP4 MAb as controls (Table 1). Both VP4 and VP6 were recognized in cells fixed with either methanol or paraformaldehyde. MAbs 1C10 and 1C3 failed to detect VP7 in virus-infected cells fixed with methanol but gave a strong positive fluorescence in cells fixed with paraformaldehyde and permeabilized with Triton X-100 (Fig. 7, Table 1).

Treatment with thapsigargin did not affect the reactivity or the pattern of recognition by MAbs against VP6 and VP4 (Fig. 7a and b). However, it induced a diminished recognition by antibodies against VP7. In the absence of thapsigargin, we observed that VP7 is recognized by the MAb, resulting in a particulate pattern of labeling extended throughout the cytoplasm (Fig. 7c). This did not occur in infected cells treated with thapsigargin, in which the intensity of fluorescence was very much decreased (Fig. 7d). Similar results were obtained with tunicamycin (Table 1). Presumably, conformational changes in VP7 could have occurred in the presence of thapsigargin, resulting in decreased recognition by the antibodies.

Effect of thapsigargin on cell death induced by infection. To study the effect of thapsigargin on the lytic effect of the virus on host cells, we measured cell permeabilization to ethidium bromide (26, 32) at different times postinfection (Fig. 8). An increase in the number of fluorescent cells began to be observed at 12 h postinfection. After this time, cell permeabilization increased until, at 15 h postinfection, all cells were fluorescent. However, cell death at this time is underestimated by this method, since the few detached dead cells were not measured. Progression of the infection on the host cell had a time course in which permeabilization to ethidium bromide preceded complete cell lysis and the release of infective viruses into the extracellular medium (26). Thapsigargin (1 μM) did not by itself induce cell death in mock-infected cells. Furthermore, it did not inhibit but rather potentiated the progression of cell death induced by virus infection. Therefore, the lytic effect is not dependent on a normal virus maturation process.

DISCUSSION

The rotavirus cycle, from penetration to the release of newly formed particles, takes place in different cellular compartments, each one characterized by a distinct Ca^{2+} concentration. As the virus enters the cell, it encounters a cytoplasmic milieu that has a Ca^{2+} concentration 10,000-fold lower than the extracellular medium (from 1 mM to 100 nM). After viral RNA and protein synthesis, the final event in the cytoplasmic stage of virus morphogenesis is thought to be the budding or transport of the single-shelled particles into the ER (13, 36), where the Ca^{2+} concentration scales up again to the millimolar order. This is the phase where the second capsid is acquired

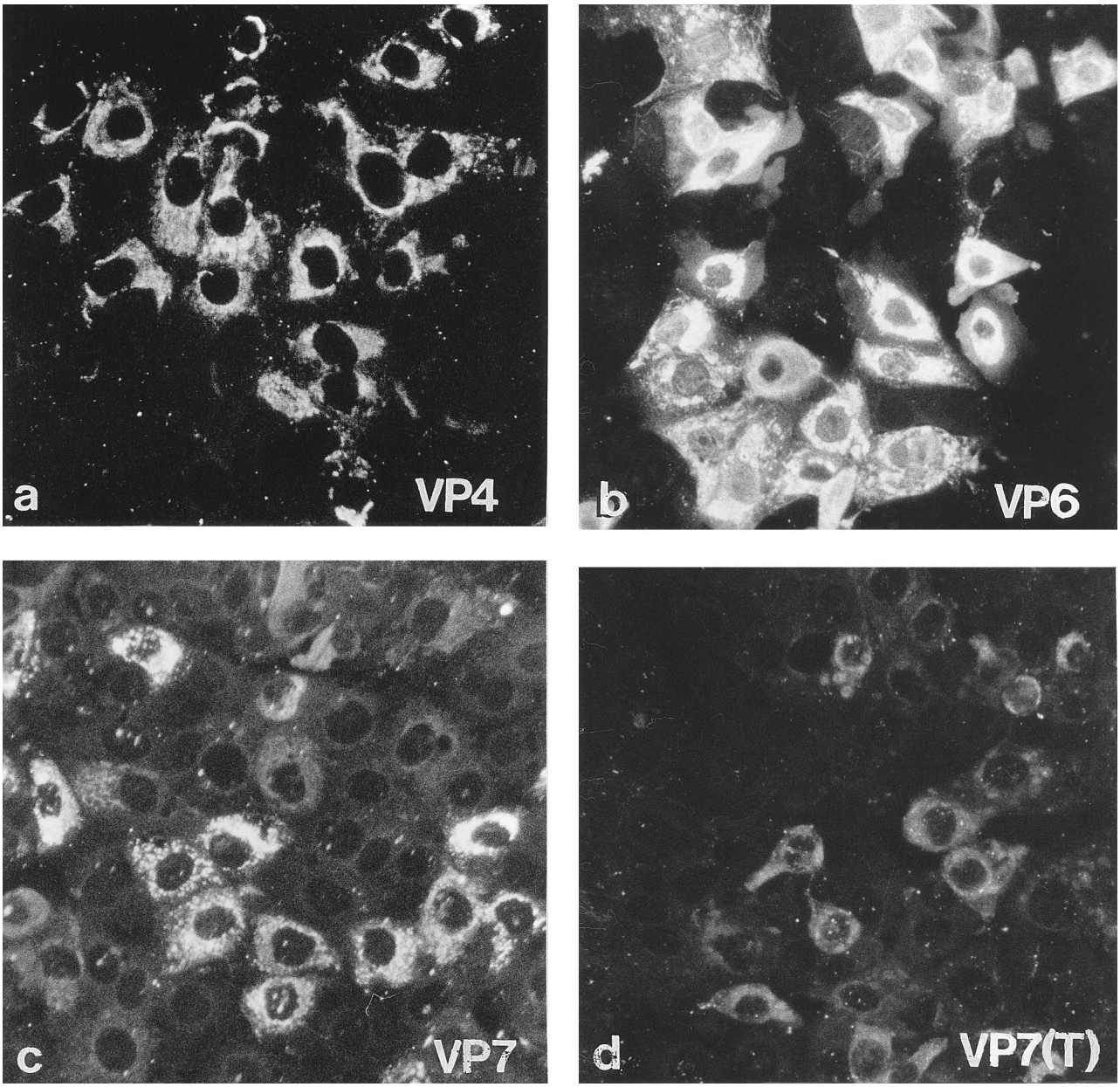

FIG. 7. Reactivity of MAbs with virus-infected MA-104 cells treated or not with thapsigargin (1 μM), as detected by immunofluorescence. Cells were grown in microtiter plates and infected with rotavirus. Thapsigargin (1 μM) was added at 1 h postinfection. At 18 h postinfection, the cells were fixed, and MAb fluorescence was developed as detailed in the text. (a) Infected cells incubated with an MAb against VP4 (5G7). (b) Infected cells incubated with an MAb against VP6 (4B2D2). (c) Infected cells incubated with an MAb against VP7 (1C10). (d) Infected cells treated with thapsigargin (1 μM) and incubated with an MAb against VP7 (1C10). Note the decreased fluorescence of cells treated with thapsigargin and labeled with the MAb against VP7 (d versus c). Thapsigargin did not affect recognition by MAbs against VP4 and VP6 (not shown). Magnification, ×2,240.

and the virus matures to its infectious form. In parallel, synthesis of viral proteins affects the Ca^{2+} homeostasis of the host cell, eventually leading to cell lysis and release of newly formed particles to the extracellular medium (26). There is a body of evidence for a link between the Ca^{2+} concentration in these different environments and the stages of the virus cycle: (i) rotaviruses need a low Ca^{2+} concentration for decapsidation (8, 14), (ii) virus maturation is blocked by total cell Ca^{2+} depletion (30), (iii) the double-capsid infectious particle is stabilized at a high-Ca^{2+} concentration (35), and (iv) the cytopathic effect is associated with the subsequent elevation in free Ca^{2+} levels in the cytoplasm (26).

Thapsigargin, by virtue of its mode of action, allows selective manipulation of the Ca^{2+} concentration within cellular compartments, allowing the evaluation of the role of different Ca^{2+} pools in virus maturation and cell death.

Thapsigargin induced a transient increase in cytoplasmic Ca^{2+} concentration and a decrease in CTC fluorescence. This was due to a passive leak from stores as a consequence of ER Ca^{2+}-ATPase inhibition (37). In this condition, the cell was

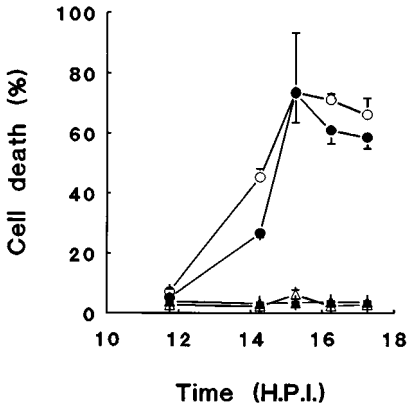

FIG. 8. Time course of cell death of infected cells in the presence or absence of thapsigargin (1 μM). Cell death was measured by permeabilization to ethidium bromide and is expressed as relative fluorescence in relation to total permeabilization by digitonin (see the text). Mock- (triangles) and virus-infected (circles) cells were treated (open symbols) or not (solid symbols) with thapsigargin. Values represent the mean ± standard error of the mean of measurements of four different wells for each condition. A representative experiment of a series of three is shown.

able to regulate this change by pumping Ca^{2+} out of the cell through the plasma membrane ATPase (3, 4). In addition, thapsigargin induced a change in Ca^{2+} permeability. This change has been explained by an activation of plasma membrane Ca^{2+} channels linked to the emptying of Ca^{2+} reservoirs of the cell (27, 31) by a mechanism which may involve the metabolism of cyclic GMP, nitric oxide, and/or cytochrome P450 (1, 41). This effect of thapsigargin on Ca^{2+} permeability was additive to that induced by rotavirus infection, suggesting the activation of two different pathways. In this sense, the complete quenching of fura2 fluorescence in rotavirus-infected cells by Mn^{2+}, in contrast to mock-infected cells, suggests that the Ca^{2+} channels activated during infection are of a different nature than those existing in the normal cell and perhaps nonphysiological.

We have shown earlier (26), and confirmed here, that rotavirus infection leads to an increase in Ca^{2+} in the intracellular deposits. These pools were released by thapsigargin, indicating that the ER is a site where Ca^{2+} is accumulated during infection. This effect of rotavirus on ER Ca^{2+} pools may be explained as the result of a primary increase in plasma membrane permeability, partially compensated for by the activation of Ca^{2+} transport into this and other compartments. However, thapsigargin affects only ER stores, whereas ionomycin releases all of them (Fig. 2).

A main conclusion that can be drawn from the effect of thapsigargin is that the elevated Ca^{2+} concentration in the cisternae of the ER is essential for rotavirus assembly and maturation. Thapsigargin did not modify the synthesis of viral proteins that takes place in the cytoplasm, but it affected the processing of viral proteins synthesized in the ER, VP7 and NS28. The change in the electrophoretic mobility of these proteins induced by thapsigargin, similar to the one induced by tunicamycin (28), is in accordance with a defect in oligosaccharide processing of NS28 and VP7 in this compartment. Unglycosylated VP7 synthesized in the presence of thapsigargin may be in a conformation that is more susceptible to degradation (33). These results confirm those obtained by Porunchynsky et al. (30), who used total intracellular Ca^{2+} depletion, and establish the role of ER-sequestered Ca^{2+} in this phase of virus morphogenesis. At variance with their experimental approach, we used conditions in which the cytoplasmic concentration of Ca^{2+} is normal or increased, suggesting a relative Ca^{2+} independence of the morphogenetic steps occurring in the cytoplasmic side of the ER. The similarity of the altered maturation outcome between thapsigargin and tunicamycin suggests that the primary event modified by ER Ca^{2+} depletion is glycosylation of the virus proteins, notably of NS28. The involvement of ER Ca^{2+} in the posttranslational processing of oligosaccharide moieties in other proteins, such as α_1-antitrypsin in HepG2 cells (2, 18–20, 40), has been described. In some cases, depletion of ER Ca^{2+} by thapsigargin and/or Ca^{2+} chelation also results in the inhibition of protein synthesis that seems to be reversed after 1 to 3 h of exposure (2, 40). In MA-104 cells, we have not detected inhibition of cell protein synthesis and have found only changes in the processing of viral glycoproteins. Perhaps after a long incubation time with thapsigargin, as we have used, an eventual early inhibition of protein synthesis could have been reversed. This has allowed us to study the role of ER Ca^{2+} in the posttranslation processing of VP7 and NS28 without affecting the initial steps of viral protein synthesis and assembly.

It has been proposed that calcium depletion blocks maturation of rotavirus by altering proper oligomerization of the viral proteins VP7, VP4, and NS28, since in cells depleted of Ca^{2+} or treated with tunicamycin, VP7 did not associate with NS28-VP4 oligomers (30).

When we probed the conformation of VP7 in thapsigargin-treated cells with a set of MAbs against VP7, we found a decreased recognition of this protein. Although no formal proof is available whether these MAbs recognize rough ER-associated or virion-complexed VP7, several characteristics of the MAbs suggest that they are directed to the virion form. First, MAbs are directed to epitopes of the major neutralization domain, which is conformation dependent; second, MAbs are unable to immunoprecipitate soluble VP7; and third, the epitopes identified are methanol sensitive (12, 17). The decreased immunofluorescence reactivity of VP7 observed in thapsigargin-treated cells could be linked to an incorrect conformation of VP7 in such particles. Furthermore, we are not sure if the in situ detergent treatment that follows paraformaldehyde fixation is effective in removing or permeabilizing the envelope, making VP7 accessible to MAbs. However, in isolated enveloped particles produced in normal conditions of infection (high Ca^{2+} in the ER), VP7 becomes accessible to protease digestion after Triton X-100 treatment (29). The change in the pattern of glycosylation and recognition of VP7 by MAbs suggests that this protein may be in a conformation other than the mature form. An alternative explanation is that the total amount of VP7 is decreased in thapsigargin-treated cells because of impaired synthesis or increased turnover (33).

Thapsigargin did not inhibit cell death induced by infection. Stored Ca^{2+} sensitive to thapsigargin does not seem to be involved in this process. The emptying of these deposits does not impair the progression of the cytopathic effect induced by infection. Thapsigargin did not inhibit the increase in Ca^{2+} permeability and concentration induced by the virus, nor did we observe with this agent a decline in the synthesis of viral proteins that takes place in the cytoplasm. These results are in accordance with our proposed model, in which an increased cytoplasmic calcium level is responsible for the lytic effect of the virus. We earlier showed that the synthesis of a viral product was required for altering intracellular Ca^{2+} homeostasis and hence inducing cell death. Blockade of the increase in cytoplasmic Ca^{2+} induced by infection by using extracellular buffers halted the cytolytic process without impairing the production of infectious particles (26).

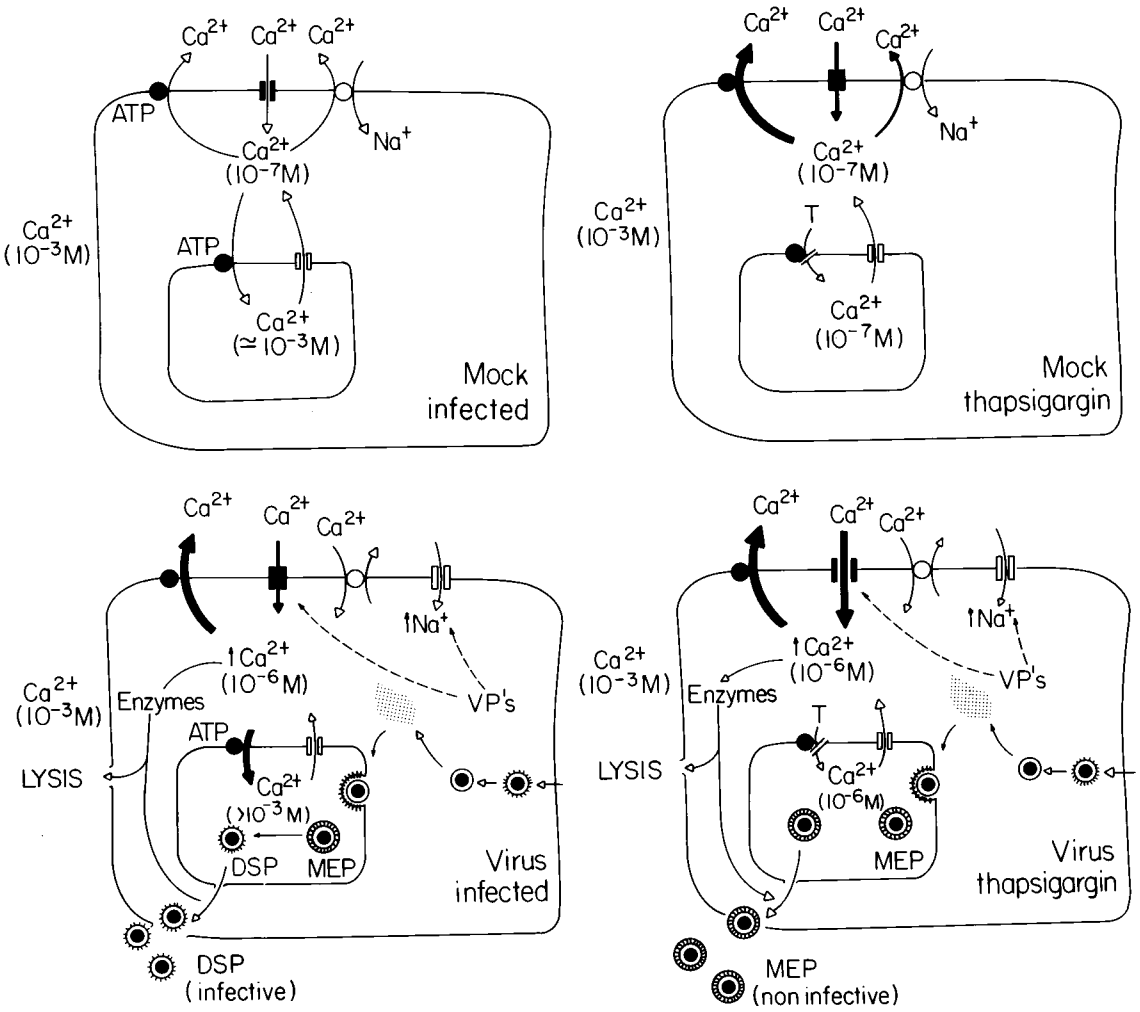

FIG. 9. Model depicting the role of different cell Ca^{2+} compartments on rotavirus maturation and the cytopathic effect evidenced by the use of thapsigargin. Normal cytosolic Ca^{2+} concentrations result from a balance between pump and leak processes occurring at the plasmalemma and the ER membrane (Ca^{2+} stores), mediated by channels and transporters (upper left). Increased Ca^{2+} movements resulting from thapsigargin treatment and/or virus infection are denoted by thick arrows. The resulting Ca^{2+} concentrations in the different compartments are shown in parentheses. The initial event in the rotavirus-infected cell that affects Ca^{2+} homeostasis is thought to be an increase in Ca^{2+} permeability of the plasma membrane that is not compensated for in spite of activated regulatory mechanisms (26). In addition to this effect, the synthesis of viral proteins (VPs) also induces a change in Na^+ permeability that eventually leads to an increase in concentration (10) and a reversal of the Na^2/Ca^{2+} exchange mechanism (lower left). Thapsigargin (T), by virtue of its inhibition of the ER Ca^{2+}-ATPase, releases Ca^{2+} from stores, with the consequent equilibration of ER Ca^{2+} concentrations with those in the cytosol. Cytosolic Ca^{2+} concentrations with thapsigargin are regulated by the plasma membrane Ca^{2+}-ATPase and the Na^+/Ca^{2+} exchange mechanism (upper right). Decreased Ca^{2+} concentrations in the ER impair the synthesis of some viral proteins and arrest rotavirus morphogenesis, with accumulation of membrane-enveloped particles (MEP) and the inhibition of the production of double-shelled particles (DSP) and hence of infectivity (lower right). The increased Ca^{2+} concentration induced by infection, which is also observed with thapsigargin, is proposed to be responsible for the activation of intracellular enzymes (proteases and phospholipases), which in turn degrade cell and membrane components, leading to cell lysis (lower left and lower right).

The viral protein(s) involved in the impairment of Ca^{2+} homeostasis and the cytopathic effect is not yet known. Recently, it has been shown that expression of recombinant NS28 in the baculovirus-insect cell system induced a sustained elevation of cytoplasmic Ca^{2+} levels in Sf9 cells. No other protein expressed resulted in this effect (39). The authors suggest that NS28 increases cytosolic Ca^{2+} levels, promoting its release from stores, and may be the protein involved in the cytopathic effect. However, if this were the case, the ER-resident protein NS28 should not allow Ca^{2+} accumulation within the ER stores. We have shown earlier and confirmed here that under normal virus replication in mammalian cultured cells, Ca^{2+} is in fact overaccumulated in this compartment. Furthermore, it is shown in this paper that a normal or high Ca^{2+} level in the ER is necessary for infectious virus maturation. The effects in insect cells may be due to the abundant expression of this protein or to a different pattern of synthesis and targeting of this protein particular to this cell type.

We present in Fig. 9 a hypothetical model depicting the role of different cell Ca^{2+} compartments in rotavirus maturation and the cytopathic effect evidenced by thapsigargin. The mechanisms intervening in the homeostasis of Ca^{2+} concentrations in the different cell compartments are stimulated during rotavirus infection, as denoted by thick arrows (26). The increased Ca^{2+} concentration in the cytoplasm (6 to 8 h postinfection) leads to activation of intracellular enzymes (proteases and phospholipases), resulting in cell necrosis and release of mature viruses. Thapsigargin, by blocking the ER Ca^{2+}-ATPase, depletes and

impairs Ca^{2+} accumulation in this compartment, arresting virus maturation at the membrane-enveloped stage. However, this agent does not affect the high levels of Ca^{2+} in the cytoplasm, linked to viral protein synthesis, which lead to cell death.

ACKNOWLEDGMENTS

This work was supported in part by grants S1-1832 and MPS-RP-IV-140031 from CONICIT, Venezuela.

We thank Jose Francisco Perez for his contribution to calcium measurements and Jean Cohen for constructive criticisms. The technical assistance of Aleida Sanchez is gratefully acknowledged. Duwhya Otero assisted with the drawings, and Mardonio Diaz assisted with the photographic work.

REFERENCES

1. **Alvarez, J., M. Montero, and J. Garcia-Sancho.** 1992. Cytochrome P450 may regulate plasma membrane Ca^{2+} permeability according to the filling state of the intracellular Ca^{2+} stores. FASEB J. **6:**786–792.
2. **Brostrom, C. O., and M. A. Brostrom.** 1990. Calcium-dependent regulation of protein synthesis in intact mammalian cells. Annu. Rev. Physiol. **52:**577–90.
3. **Carafoli, E.** 1987. Intracellular calcium homeostasis. Annu. Rev. Biochem. **56:**395–433.
4. **Carafoli, E.** 1992. The Ca^{2+} pump of the plasma membrane. J. Biol. Chem. **267:**2115–2118.
5. **Caswell, A. H., and J. D. Hutchison.** 1971. Visualization of membrane bound cations by a fluorescent technique. Biochem. Biophys. Res. Commun. **42:** 43–49.
6. **Chandler, D. E., and J. A. Williams.** 1978. Intracellular divalent cation release in pancreatic acinar cells during stimulus-secretion coupling: use of chlorotetracycline as fluorescent probe. J. Cell Biol. **76:**371–385.
7. **Ciarlet, M., and F. Liprandi.** Unpublished results.
8. **Cohen, J., J. Laporte, A. Charpilienne, and R. Scherrer.** 1979. Activation of rotavirus RNA polymerase by calcium chelation. Arch. Virol. **60:**177–186.
9. **Del Castillo, J. R., J. E. Ludert, A. Sanchez, M. C. Ruiz, F. Michelangeli, and F. Liprandi.** 1991. Rotavirus infection alters Na^+ and K^+ homeostasis in MA-104 cells. J. Gen. Virol. **72:**541–547.
10. **Dixon, D., N. Brandt, and D. H. Haynes.** 1984. Chlorotetracycline fluorescence is a quantitative measure of the free internal Ca^{2+} concentration achieved by active transport. J. Biol. Chem. **259:**13737–13741.
11. **Dormitzer, P. R., and H. B. Greenberg.** 1992. Calcium chelation induces a conformational change in recombinant herpes simplex virus-1-expressed rotavirus VP7. Virology **189:**828–832.
12. **Dormitzer, P. R., D. Y. Ho, E. R. Mackow, E. S. Mocarski, and H. B. Greenberg.** 1992. Neutralizing epitopes on herpes simplex virus-1-expressed rotavirus VP7 are dependent on coexpression of other rotavirus proteins. Virology **187:**18–32.
13. **Estes, M. K.** 1991. Rotaviruses and their replication, p. 619–642. *In* B. N. Fields, D. M. Knipe, et al. (ed.), Fundamental virology. Raven Press, New York.
14. **Estes, M. K., D. Y. Graham, E. M. Smith, and C. P. Gerba.** 1979. Rotavirus stability and inactivation. J. Gen. Virol. **43:**403–409.
15. **Gorziglia, M., C. Larrea, F. Liprandi, and J. Esparza.** 1985. Biochemical evidence of the oligomeric (possibly trimeric) structure of the major inner capsid polypeptide (45 K) of rotaviruses. J. Gen. Virol. **66:**1889–1900.
16. **Grynkiewicz, G., M. Poenie, and R. Y. Tsien.** 1985. A new generation of Ca^{2+} indicators with greatly improved fluorescence properties. J. Biol. Chem. **260:**3440–3450.
17. **Kabcenell, A. K., M. S. Poruchynsky, A. R. Bellamy, H. B. Greenberg, and P. H. Atkinson.** 1988. Two forms of VP7 are involved in assembly of SA11 rotavirus in endoplasmic reticulum. J. Virol. **62:**2929–2941.
18. **Kuznetsov, G., M. A. Brostrom, and C. O. Brostrom.** 1992. Demonstration of calcium requirement for secretory protein processing and export: differential effects of calcium and dithiothreitol. J. Biol. Chem. **267:**3932–3939.
19. **Kuznetsov, G., M. A. Brostrom, and C. O. Brostrom.** 1993. Role of endoplasmic reticular calcium in oligosaccharide processing of α^1-antitrypsin. J. Biol. Chem. **268:**2001–2008.
20. **Liprandi, F., G. Lopez, I. Rodriguez, M. Hidalgo, J. E. Ludert, and N. Mattion.** 1990. Monoclonal antibodies to the VP6 of porcine subgroup I rotaviruses reactive with subgroup I and non-subgroup II strains. J. Gen. Virol. **71:**1395–1398.
21. **Liprandi, F., I. Rodriguez, C. Pina, G. Larralde, and M. Gorziglia.** 1991. VP4 monotype specificities among porcine rotavirus strains of the same VP4 serotype. J. Virol. **65:**1658–1661.
22. **Lodish, H. F., and N. Kong.** 1990. Perturbation of cellular calcium blocks exit of secretory proteins from the rough endoplasmic reticulum. J. Biol. Chem. **265:**10893–10899.
23. **Mass, D. R., and P. H. Atkinson.** 1990. Rotavirus proteins VP7, NS28, and VP4 form oligomeric structures. J. Virol. **64:**2632–2641.
24. **Merritt, J. E., and T. J. Hallam.** 1988. Platelets and parotid acinar cells have different mechanisms for agonist-stimulated divalent cation entry. J. Biol. Chem. **263:**6161–6164.
25. **Michelangeli, F., and M. C. Ruiz.** 1984. Ca^{2+} as modulator of gastric secretion and vesicular H^+ transport, p. 149–159. *In* J. G. Forte, D. Warnock, and F. C. Rector, Jr. (ed.), Hydrogen ion transport in epithelia. Wiley-Interscience, New York.
26. **Michelangeli, F., M. C. Ruiz, J. R. del Castillo, J. E. Ludert, and F. Liprandi.** 1991. Effect of rotavirus infection on intracellular calcium homeostasis in cultured cells. Virology **181:**520–527.
27. **Montero, M., J. Alvarez, and J. Garcia-Sancho.** 1991. Agonist-induced Ca^{2+} influx in human neutrophils is secondary to the emptying of intracellular calcium stores. Biochem. J. **277:**73–79.
28. **Petrie, B. L., M. K. Estes, and D. Y. Graham.** 1993. Effects of tunicamycin on rotavirus morphogenesis and infectivity. J. Virol. **46:**270–274.
29. **Poruchynsky, M. S., and P. H. Atkinson.** 1991. Rotavirus protein rearrangements in purified membrane-enveloped intermediate particles. J. Virol. **65:** 4720–4727.
30. **Poruchynsky, M. S., D. R. Mass, and P. H. Atkinson.** 1991. Calcium depletion blocks the maturation of rotavirus by altering the oligomerization of virus-encoded proteins in the ER. J. Cell Biol. **114:**651–661.
31. **Putney, J. W., Jr.** 1986. A model for receptor-regulated calcium entry. Cell Calcium **7:**1–12.
32. **Ruiz, M. C., F. Michelangeli, J. E. Ludert, F. Liprandi, J. R. del Castillo, M. E. Chemello, G. Benaim, and E. Cohen.** 1991. Fluorimetric quantification of cell death in monolayer cultures and cell suspensions. J. Biochem. Biophys. Methods **23:**237–248.
33. **Shahrabadi, M. S., L. A. Babiuk, and P. W. K. Lee.** 1987. Further analysis of the role of calcium in rotavirus morphogenesis. Virology **158:**103–111.
34. **Shahrabadi, M. S., and P. W. K. Lee.** 1986. Bovine rotavirus maturation is a calcium-dependent process. Virology **152:**298–307.
35. **Shirley, J. A., G. M. Beards, M. E. Thouless, and T. H. Flewett.** 1981. The influence of divalent cations on the stability of human rotavirus. Arch. Virol. **67:**1–9.
36. **Suzuki, H., T. Konno, and Y. Numazaki.** 1993. Electron microscopic evidence for budding process-independent assembly of double-shelled rotavirus particles during passage through endoplasmic reticulum membranes. J. Gen. Virol. **74:**2015–2018.
37. **Thastrup, O.** 1990. Role of Ca^{2+}-ATPases in regulation of cellular Ca^{2+} signalling, as studied with the selective microsomal Ca^{2+}-ATPase inhibitor, thapsigargin. Agents Actions **29:**8–15.
38. **Thastrup, O., A. P. Dawson, O. Scharff, B. Foder, P. J. Cullen, B. K. Drobak, P. J. Bjerrum, S. B. Christensen, and M. R. Hanley.** 1989. Thapsigargin, a novel molecular probe for studying intracellular calcium release and storage. Agents Actions **27:**17–23.
39. **Tian, P., Y. Hu, W. P. Schilling, D. A. Lindsay, J. Eiden, and M. K. Estes.** 1994. The nonstructural glycoprotein of rotavirus affects intracellular calcium levels. J. Virol. **68:**251–257.
40. **Wong, W. L., M. A. Brostrom, G. Kuznetsov, D. Gmitter-Yellen, and C. O. Brostrom.** 1993. Inhibition of protein synthesis and early protein processing by thapsigargin in cultured cells. Biochem. J. **289:**71–79.
41. **Xu, X., R. A. Star, G. Tortorici, and S. Muallem.** 1994. Depletion of intracellular Ca^{2+} stores activates nitric-oxide synthase to generate cGMP and regulate Ca^{2+} influx. J. Biol. Chem. **269:**12645–12653.